A Weight Function for Zr-2.5Nb Pressure Tube Burst Test Specimens

(DRAFT FOR REVIEW)

Steven X. Xu*, Douglas A. Scarth

Structural Integrity and Risk Assessment, Kinectrics Inc., Toronto M8Z 5G5, Canada
* Corresponding author: steven.xu@kinectrics.com

Abstract Based on a literature review, the weight function for an axial through-wall crack in a cylinder has not been reported in the open literature. A weight function for an axial through-wall crack in a cylinder that is applicable to the pressure tube burst test specimens has been developed and is described in this paper. Three-dimensional finite element analyses were performed to calculate the stress intensity factors corresponding to line loads on the crack face. The calculated stress intensity factors were used to develop a weight function for the pressure tube burst test specimens based on regression analysis and engineering judgment.

Keywords Weight function, Stress intensity factor, Axial through-wall crack, Pressure tube, Burst test

1. Introduction

In CANDU® nuclear reactors, the primary containment for the uranium dioxide fuel is provided by thin-walled Zr-2.5Nb pressure tubes, which are nominally 6.3 m long, 103 mm in diameter, and 4.2 mm thick [1, 2]. During operation, the pressure tubes undergo corrosion with the heavy water coolant, D_2O. A portion of the deuterium (D) released by the corrosion reaction is absorbed by the pressure tube and its accumulation over time represents a primary integrity concern. Technical requirements for in-service evaluation of Zr-2.5Nb pressure tubes in CANDU reactors are provided in the CSA Standard N285.8 [3], including evaluation of service conditions for protection against fracture of operating pressure tubes, as well as defense-in-depth demonstration of leak-before-break. Evaluation procedures for protection again fracture and demonstration of leak-before-break are based on use of the fracture toughness versus temperature relationship. Fracture toughness measurements from pressure tube burst tests have shown that hydrides associated with high levels of hydrogen equivalent concentrations can have a significant effect on reducing the fracture toughness at reactor operating temperature during reactor warm-up and cool-down [4]. To support safe operation of pressure tubes at late life where the projected hydrogen equivalent concentrations are of high levels, there has been an initiative in CANDU industry in Canada to gain mechanistic understanding of the effect of levels of hydrogen equivalent concentrations on fracture toughness. A cohesive-zone based engineering fracture toughness model is being developed to assess the effect of zirconium hydrides on the fracture toughness of Zr-2.5 Nb pressure tubes. The knowledge of weight function is required in the calculation of crack opening displacement in the cohesive-zone modeling. Based on a literature review, the weight function for an axial through-wall crack in a cylinder has not been reported in the open literature. A weight function for an axial through-wall crack in a cylinder that is applicable to the Zr-2.5Nb pressure tube burst test specimens have been developed and is described in this paper.

2. Considerations for Development of Weight Function for Burst Test Specimens

A schematic illustration of the pressure tube burst test specimen is given in Figure 1. Three-dimensional finite element analyses were performed to calculate the stress intensity factors corresponding to line loads on the crack face. The calculated stress intensity factors were used to develop a weight function for the burst test specimens based on regression analysis and engineering

® CANDU is a registered trademark of Atomic Energy of Canada Ltd.

judgment**.** The following considerations for the development of a weight function for the burst test specimens were identified.

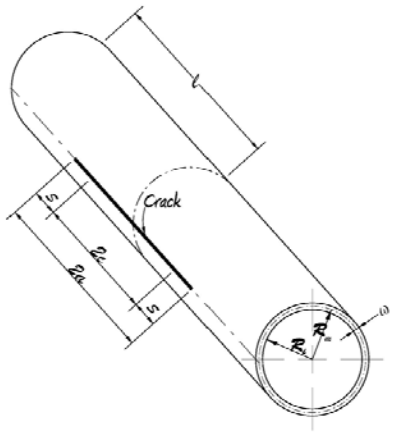

Figure 1. Illustration of pressure tube burst test specimen

(1) Consideration was given to ranges of dimensions for the burst test specimens. Variations in inner radius R_i and wall thickness w of pressure tube burst test specimens are insignificant. The dimension ranges for pressure tube inner radius and wall thickness were not considered. A representative inner radius R_i = 52 mm and wall thickness w = 4.0 mm were used in the weight function development. The initial crack length of a burst test specimen, $2c$, is typically 55 mm. An axial through-wall crack with length $2a$ of 50 to 75 mm was considered in the weight function development.

(2) Consideration was given to the crack model as one dimensional. The axial through-wall crack was treated as one dimensional, and the crack geometry was characterized by the crack length. The treatment of a one-dimensional crack in the axial direction of the pressure tube is considered to be reasonable since the ratios of pressure tube radius to wall thickness of burst test specimens exceed ten. The overall behavior of a pressure tube burst test specimen is expected to be representative of a plane stress state. This assumption was verified through finite element calculations as described in Section 3.

(3) Consideration was given to characterization of the crack-tip singularity. It was assumed that a through-wall axial crack in a pressure tube and a through-wall crack in a flat plate have the same type of singularity. This assumption forms the basis for the proposed format for the weight function for the burst test specimens. Using the notation as illustrated in Figure 2, one format of the weight function for a through-wall crack in an infinite flat plate, $m_0(x,a)$, is given by Eq. 1 [5].

$$m_0(x,a) = \frac{2}{\sqrt{\pi a}} \frac{1}{\sqrt{1-\left(\frac{x}{a}\right)^2}} \tag{1}$$

where x is x-coordinate relative to the crack center in an infinite plate.

(4) Consideration was given to the format of the weight function for the burst test specimens. Further to the consideration in (3), it was assumed that the weight function for an axial through-wall crack in a pressure tube, $m(x,a)$, can be written in terms of the weight function for a through-wall crack in an infinite flat plate with a modification coefficient. It is assumed that the modification coefficient is a function of the location parameter x/a, and the geometry parameter $a/\sqrt{R_m w}$, as expressed in Eq. 2. This assumption is based on engineering judgment. As discussed later in Sections 4 and 5, finite element calculation results provided support for this assumption.

$$m(x,a) = m_0(x,a)\, F\left(\frac{x}{a}, \frac{a}{\sqrt{R_m w}}\right) \tag{2}$$

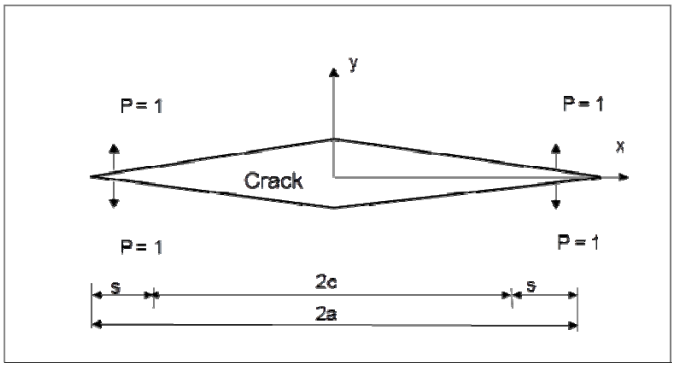

Figure 2. Weight function notation for a central through-wall crack
in a flat plate or an axial crack in a pressure tube

3. Confirmation of Thickness Averaged Behavior of Plane Stress State

Three-dimensional elastic finite element analyses were performed to calculate the stress intensity factors for an axial through-wall crack in an internally pressurized long cylinder. The geometry of a representative burst test specimens was used. The inner radius of the cylinder was R_i = 52 mm and wall thickness was w = 4.0 mm. Two cases of crack length were considered, $2a$ = 50 mm and $2a$ = 75 mm. The length of the cylinder was set to 50 times crack length in the finite element model. Crack face pressure loading was included. Only one quarter of the cylinder was modeled and analyzed due to the symmetry consideration. The fracture mechanics specific three-dimensional finite element mesh generation tool FEACrack was used [6]. The generated three-dimensional finite element mesh for a 50 mm long axial through-wall crack is shown in Figure 3. The mesh contains 107,246 nodes and 24,360 20-node brick elements. Twenty one elements were used across the wall thickness near the crack-tips. The spider-web mesh design was used with concentric rings of elements focused towards the crack tips. The element edge length for the first ring elements was 5 μm. The mid-side nodes at the crack-tips were move to the one-quarter points. The crack-tip nodes were tied together. A similar mesh was used for the case of a 75 mm long crack. The mesh for the 75 mm long crack contains 119,446 nodes and 26,985 20-node brick elements. Elements around the crack-tips were essentially the same as in the case of 50 mm long crack.

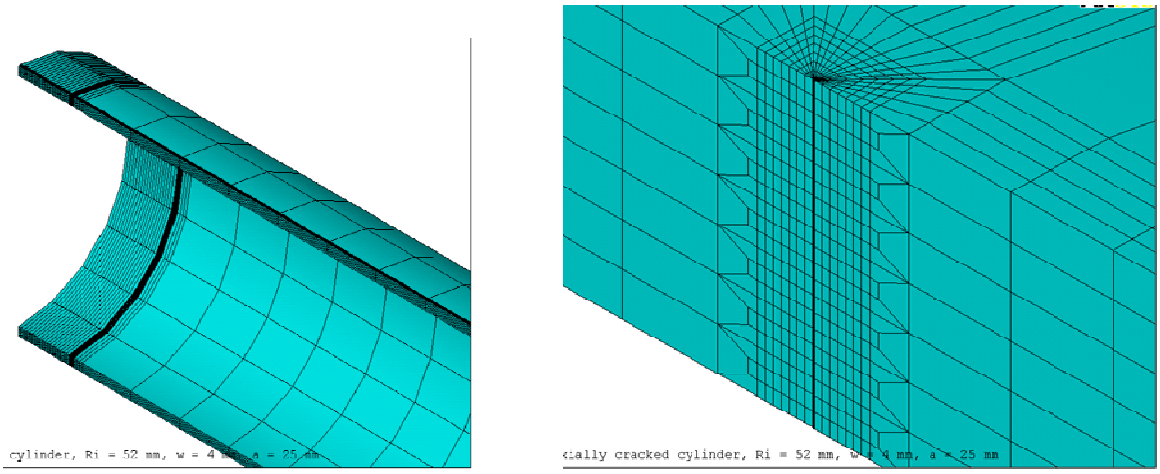

Figure 3. Three-dimensional finite element mesh of one quarter of a pressure tube burst test specimen

Two cases of Poisson's ratio were considered, $\upsilon = 0.3$ and $\upsilon = 0.4$. Finite element analyses were performed using ANSYS [7]. Stress and strain data obtained from ANSYS were read to FEACrack for calculation of the J integral. The path independence of J integral results was confirmed. Forty-three values of the J integral were obtained along the wall thickness for each case of crack depth and Poisson's ratio. Each value of J was converted to a stress intensity factor, K_I, using either plane stress or plane strain conditions. An internal pressure of p = 100 MPa was used in the calculation, with inclusion of crack face pressure. Since the calculations are based on linear elastic material behavior, the level of internal pressure is arbitrary in the context of development of weight functions. The thickness averaged K_I results for crack length $2a$ of 50 and 75 mm for plane stress and plane strain conditions, when Poisson's ratio $\upsilon = 0.3$ was used in the finite element calculations, are listed in Table 1. The mid-thickness K_I results are also listed for comparison. In addition, the K_I results calculated based on the commonly used bulging factor are listed in Table 1 [3]. The bulging factor is based on the shallow shell theory and calculated K_I results correspond to plane-stress conditions [8, 9, 10]. It is seen that the thickness averaged K_I results for plane stress conditions are in reasonable agreement with the K_I results calculated based on the bulging factor. The mid-thickness K_I results also generally agree with K_I results calculated based on the bulging factor, but the agreement is not as good as the thickness averaged K_I results. Similarly, the thickness averaged K_I results and the mid-thickness K_I results when Poisson's ratio $\upsilon = 0.4$ was used in the finite element calculations are listed in Table 2. The K_I results calculated based on the bulging factor are also listed in Table 2. Again, it is seen that the thickness averaged K_I results for plane-stress conditions are in reasonable agreement with the K_I results calculated based on the bulging factor.

The above observations from Tables 1 and 2 confirm that the thickness averaged behavior of the pressure tube is of a plane stress state. This average over the wall thickness approach was subsequently used to extract stress intensity factor results from three-dimensional finite element results for the development of the weight function for the burst test specimens as described in Sections 4 and 5.

Another observation from Tables 1 and 2 is that the effect of Poisson's ratio on the thickness averaged K_I results for plane-stress conditions is insignificant. In Table 1 with $\upsilon = 0.3$, the thickness averaged K_I are 854 and 1406 MPa√m for crack lengths $2a$ = 50 and 75 mm, respectively. In Table 2 with $\upsilon = 0.4$, the corresponding K_I are 849 and 1398 MPa√m for crack lengths $2a$ = 50 and 75 mm, respectively. This observation provides additional support for using the wall thickness averaged result when extracting three-dimensional finite element results for the development of the weight function for burst test specimens.

Table 1. Stress intensity factors for an axial through-wall crack in a pressure tube with internal pressure of 100 MPa, Poisson's ratio of 0.3 used in finite element calculation

METHOD TO CALCULATE STRESS INTENSITY FACTOR		STRESS INTENSITY FACTOR, K_I (MPa√m)	
		$2a$ = 50 mm	$2a$ = 75 mm
Averaged result over thickness based on 3-D FE results	Plane stress	854 MPa√m	1406 MPa√m
	Plane strain	895 MPa√m	1474 MPa√m
Mid-thickness result based on 3-D FE results	Plane stress	874 MPa√m	1441 MPa√m
	Plane strain	917 MPa√m	1511 MPa√m
Result based on the bulging factor [3]		834 MPa√m	1409 MPa√m

Table 2. Stress intensity factors for an axial through-wall crack in a pressure tube with internal pressure of 100 MPa, Poisson's ratio of 0.4 used in finite element calculation

METHOD TO CALCULATE STRESS INTENSITY FACTOR		STRESS INTENSITY FACTOR, K_I (MPa√m)	
		$2a$ = 50 mm	$2a$ = 75 mm
Averaged result over thickness based on 3-D FE results	Plane stress	849 MPa√m	1398 MPa√m
	Plane strain	927 MPa√m	1526 MPa√m
Mid-thickness result based on 3-D FE results	Plane stress	882 MPa√m	1455 MPa√m
	Plane strain	962 MPa√m	1587 MPa√m
Result based on the bulging factor [3]		834 MPa√m	1409 MPa√m

4. Finite Element Calculation of Weight Function for Burst Test Specimens

A one-dimensional weight function can be interpreted as the stress intensity factor for a pair of opposing unit line loads acting on the crack faces of a three-dimensional cracked body. Three-dimensional finite element analyses were performed to calculate the stress intensity factors for a line load on the crack faces, or discrete values of the weight function, for pressure tube burst test specimens.

As discussed in Considerations (3) and (4) in Section 2, it was assumed that the normalized weight function for the pressure tube burst test specimen, $m(x,a)/m_0(x,a)$, does not contain any singularity, where $m_0(x, a)$ is the weight function for a through-wall crack in an infinite flat plate. It was also assumed that the normalized weight function $m(x,a)/m_0(x,a)$ is a function of the location parameter x/a and the geometry parameter $a/\sqrt{R_m w}$.

Table 3. Finite element calculation matrix for development of weight function for burst test specimen

CALCULATION SET	CRACK LENGTH, $2a$ (mm)	LOAD LOCATION, x/a
I	12 values distributed between [2, 100]	0
II	50	10 values distributed between [0, 1)
III	75	10 values distributed between [0, 1)

The finite element calculation matrix for the development of a weight function for the burst test specimens is listed in Table 3. The pressure tube inner radius R_i of 52 mm and wall thickness w of 4.0 mm were used in all cases. Poisson's ratio $\upsilon = 0.3$ was used. Based on the discussion in Section 3, the effect of Poisson's ratio on the wall thickness averaged K_I values for plane-stress conditions has been confirmed to be insignificant. Three sets of finite element calculations in Table 3 were chosen based on parameter combinations of load location and crack length. In calculation Set-I, the load was always applied on the crack center line, *i.e.* $x/a = 0$. Discrete values of the weight function from calculation Set-I were used to characterize the trend of the weight function with the geometry parameter $a/\sqrt{R_m w}$. In calculation Set-II, the crack length was fixed to $2a$ = 50 mm, and pressure load was applied to lines located at ten different locations between crack centers and crack-tips.

Calculation Set-III is similar to Set-II, except that the crack length was $2a$ = 75 mm. The finite element mesh design was the same as described in Section 3. An example of a crack-tip zoomed-in view of the three-dimensional finite element mesh of one quarter of a burst test specimen with line load of pressure applied on the crack face is given in Figure 4.

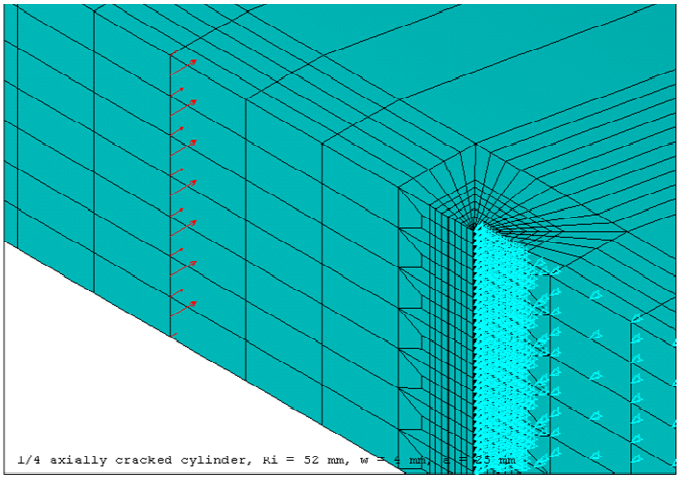

Figure 4. Crack-tip zoomed-in view of three-dimensional finite element mesh of one quarter of a pressure tube burst test specimen with inner radius of 52 mm, wall thickness of 4 mm, and 50 mm long axial through-wall crack, line load of pressure applied on crack face (denoted by red arrows)

The wall thickness averaged K_I results for plane-stress conditions, or the discrete values of weight function $m(x, a)$, were extracted from the three-dimensional finite element results. The normalized weight functions $m(x,a)/m_0(x,a)$ were obtained for the calculation Sets-I, II and III, respectively.

5. Regression Fit and Proposed Weight Function

The wall thickness averaged finite element results of normalized weight function obtained in Section 4 were fitted to an engineering equation using TableCurve2D [11], in conjunction with engineering judgment.

The discrete values of normalized weight function at the crack center for the calculation Set-I in Table 3 were found to fit well with the following simple equation.

$$\frac{m(0,a)}{m_0(0,a)} = \sqrt{1+3.696\frac{a^2}{R_m w}} \tag{3}$$

The R^2 coefficient of variation was 0.999, the fit standard error was 0.0612, and F-statistic was 11570. The comparison of finite element data and the fitted equation is plotted in Fig. 5. The maximum fitting error was 2.1%.

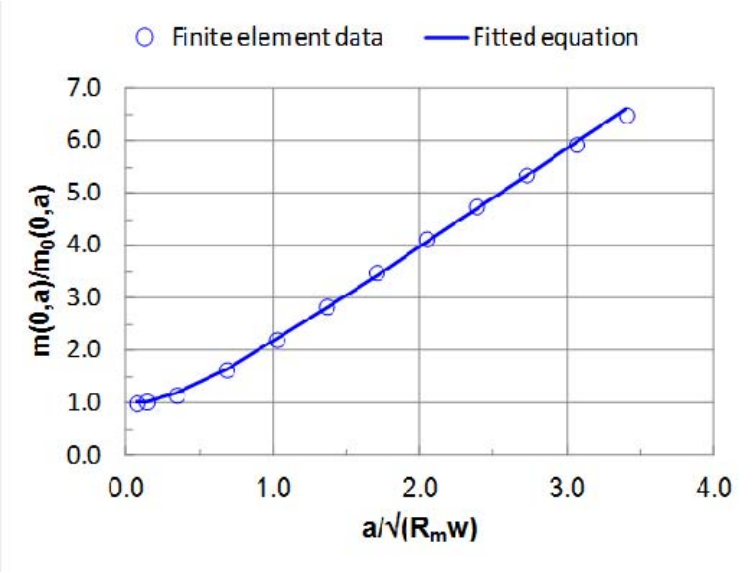

Figure 5. Finite element results and fitted equation of normalized weight function for the calculation Set-I for an axial through-wall crack in a pressure tube

The trend of normalized weight function with the location parameter *x/a* was investigated using the finite element data for the calculation Set-II and Set-III in Table 3. The discrete values of normalized weight function $m(x,a)/m_0(x,a)$ for a crack length of $2a$ = 50 mm for the calculation Set-II were fitted as a function of *x/a*. A separate fit was performed for the data for the calculation Set-III for a crack length of $2a$ = 75 mm. It was found that the equation format of Eq. (4) fits well to the data for both calculation sets. For the case of the 50 mm long crack, the fit standard error was 0.0371, and the *F*-statistic was 3635. For the case of the 75 mm long crack, the fit standard error was 0.0478, and the *F*-statistic was 6160.

$$\frac{m(x,a)}{m_0(x,a)} = C_1 + C_2\left(\frac{x}{a}\right)^2 \tag{4}$$

where C_1 and C_2 are fitting coefficients.

The fitting of C_1 and C_2 in Eq. (4) were used to determine the appropriate functional form of $m(x,a)/m_0(x,a)$, and were not used in the final form of the weight function. In the absence of using a three-dimensional fitting tool and with limited finite element data, engineering judgment was applied to establish an engineering equation using equation formats of Eqs. (3) and (4). The engineering equation is written as

$$\frac{m(x,a)}{m_0(x,a)} = M - (M-1)\left(\frac{x}{a}\right)^2 \tag{5}$$

with

$$M = \sqrt{1 + 3.696\frac{a^2}{R_m w}} \tag{6}$$

The comparison of finite element data for the calculation Set-II and Sec-III and the engineering equations of Eqs. (5) and (6) is plotted in Figure 6. The maximum fitting error was 4.2% for the data for the calculation Set-II, and 6.7% for the data for the calculation Set-III. These fitting errors were considered to be acceptable. An improved equation fit might be obtained if a proper three-dimensional fitting tool was used in the fitting process. Generating additional finite element data for crack lengths other than $2a$ = 50 and 75 mm may be necessary for improvement in the equation fit.

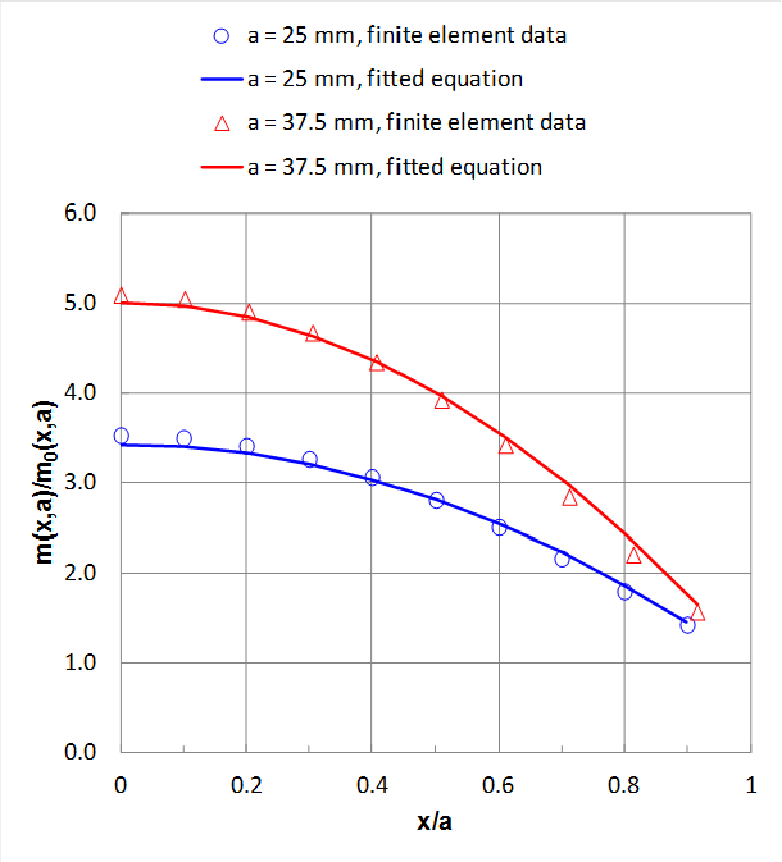

Figure 6. Finite element results and fitted equation of normalized weight function for calculation Set-II and Set-III for an axial through-wall crack in a pressure tube

The proposed weight function for the burst test specimen is given by

$$m(x,a)=\frac{2}{\sqrt{\pi a}}\frac{1}{\sqrt{1-\left(\frac{x}{a}\right)^2}}\left[M-(M-1)\left(\frac{x}{a}\right)^2\right] \tag{7}$$

where the parameter M is given by Eq. (6).

It is reasonable to expect that, when loading on the crack face is uniform, the stress intensity factor calculated using the developed weight function is consistent with the conventional calculation approach based on the bulging factor for an axial through-wall crack. This consistence was checked. When the internal pressure is p, the stress intensity factor for the burst test specimen using the

bulging factor M_b, $K_I(M_b)$, is written as Eqs. (8) and (9).

$$K_I(M_b) = p\frac{R_i}{w}M_b\sqrt{\pi a} \tag{8}$$

with

$$M_b = \sqrt{1+1.255\frac{a^2}{R_m w}-0.0135\left(\frac{a^2}{R_m w}\right)^2} \tag{9}$$

With the use of the weight function approach, the stress intensity factor for the burst test specimens, $K_I(m)$, is written as

$$K_I(m) = \int_0^a m(x,a)\, p\frac{R_i}{w}dx \tag{10}$$

Substitution of Eq. (7) into Eq. (10) results in

$$K_I(m) = p\frac{R_i}{w}\left(\frac{M+1}{2}\right)\sqrt{\pi a} \tag{11}$$

The numerical values of $K_I(M_b)$ and $K_I(m)$ were compared for four cases of crack length, $2a$ = 50, 60, 75 and 100 mm. The percentage differences between $K_I(M_b)$ and $K_I(m)$ are within 5%.

Acknowledgements

This work was funded by the CANDU Owners Group.

References

[1] W.J. Langford, L.E.J. Mooder, Fracture behaviour of zirconium alloy pressure tubes for Canadian nuclear power reactors. International Journal of Pressure Vessels and Piping, 6 (1978) 275–310.
[2] P.H. Davies and R.S.W. Shewfelt, Link Between Results of Small- and Large-Scale Toughness Tests on Irradiated Zr-2.5Nb Pressure Tube Material, in: E.R. Bradley and G.P. Sabol (Eds.), Zirconium in the Nuclear Industry: Eleventh International Symposium, ASTM STP 1295, American Society for Testing and Materials, 1996, 492-517.
[3] Canadian Standards Association, Technical Requirements for In-service Evaluation of Zirconium Alloy Pressure Tubes in CANDU Reactors, CSA Standard N285.8-10, Toronto, 2010.
[4] S. St Lawrence, unpublished work, 2012.
[5] G. Glinka and G. Shen, Universal Features of Weight Functions for Cracks in Mode I. Engineering Fracture Mechanics, 40 (1991) 1135-1146.
[6] FEACRACK, 3D Finite Element Software for Cracks, Version 3.2.16, Quest Reliability, Boulder, CO, U.S.A., 2012.
[7] ANSYS, General Purpose Finite Element Software, ANSYS Mechanical, Version 14.0, Ansys, Canonsburg, Pennsylvania, U.S.A., 2012.
[8] E.S. Folias, An Axial Crack in a Pressured Cylindrical Shell. International Journal of Fracture Mechanics, 1 (1965) 104-113.
[9] R. Ehlers, Stress Intensity Factors and Crack Opening Areas for Axial Through Cracks in Hollow Cylinders under Internal Pressure Loading. Engineering Fracture Mechanics, 25 (1986) 63-77.
[10] J.F. Kiefner, W.A. Maxey R.J. Eiber and A.R. Duffy, Failure Stress Levels of Flaws in Pressurized Cylinders. ASTM STP 536, 1973, 461-481.
[11] TableCurve 2D, Automated Curve Fitting Software, Version 5.01, SYSTAT Software Inc., Richmond, CA, U.S.A., 2002.